16th World Conference on Earthquake Engineering, 16WCEE 2017

Santiago Chile, January 9th to 13th 2017

Paper N° 3853

Registration Code: S-R1464283307

Geophysical study and 3D modeling of site effects in the basin of Marga Marga, Viña del Mar, Chile.

L. Podestá [1,3], E. Sáez [2,3].

[1] *MSc. student, Departamento de Estructuras y Geotecnia, Pontificia Universidad Católica de Chile, lfpodesta@uc.cl*

[2] *Associate Professor, Departamento de Estructuras y Geotecnia, Pontificia Universidad Católica de Chile, esaez@ing.puc.cl*

[3] *Center for Integrated Natural Disaster Management CONICYT/FONDAP/15110017, Chile.*

Abstract

The February 27, 2010 earthquake has induced damage to several buildings in the entire area of central Chile. Particularly in the Marga Marga basin, an anomalous concentration of structural damage was found in the downtown area of Viña del Mar city. Indeed, extensive damage was found in several medium-height buildings distributed along a narrow area of approximately 1 km in length. These observations suggest the existence of localized seismic amplification effects. A geophysical characterization using Surface-Waves based techniques and gravimetry was conducted to characterize the main dynamic properties of the soil and the depth of the basin. These data were complemented with several Standard Penetration Test (SPT) measurements to develop a 3D geotechnical characterization of the area. Based on this geotechnical description, a computational 3D model was developed to estimate possible site amplification effects explaining that concentration of structural damage. Initial results are in good agreement with damage observations and suggest an explanation related to basement shape.

Keywords: Site effects; Numerical modeling; Geophysical survey.

1. Introduction

As it is well known, Chile is one of the most seismic countries in the world, largely due to subduction of the Nazca plate beneath the South American plate. In Chile, it is possible to expect approximately one important earthquake each ten years [1]. Particularly, the central area of Viña del Mar, historically known as Población Vergara, suffered considerable damage in the 1906 and 1985 earthquakes; both of them, had the epicenter in the coast of Chile's Region V. In contrast, the adjacent uplands areas, which are underlain by metamorphic and granitic rocks, were relatively undamaged [2]. More recently, structural damage in almost 9 medium-height buildings [3] was reported in the same zone of Viña del Mar for the February 27, 2010 earthquake, located at more than 400 km from epicenter.

One of the factors that contributes most to damages in urban areas is the proximity to the hypocenter; but in this case, it's more intuitive to attribute it to soil amplification effects. This effect can explain a bounded damage zone during an earthquake, where the local morphology and geology are crucial [4]. Thus, to characterize the central area of Viña del Mar, we used geophysical methods based on surface-waves and gravity measurements, with the main purpose to obtain a basement geometry of the valley and the soil's dynamic parameters, to allow us to model complex site effects.

Chilean current seismic design code for residential buildings classifies the entire studied zone as having a type D soil (according to 180<Vs30<350 m/s and SPT blow counts). This means that the design of all buildings is subject to the same design acceleration spectrum. Nevertheless, damage concentration suggests that acceleration levels are not uniform through this zone of the city.

2. Geological setting and damaged buildings

The studied area is located in the downtown of the city of Viña del Mar, Chile (33°01'30"S 71°33'9"O WGS84). Specifically, the littoral sector of the valley, crossed by the Marga Marga river. The geology of this valley is characterized by fluvial unconsolidated sediments (Qf), composed of sand, silt and, to a minor extent, gravel. The Northern limits of this unit are hills of variable heights, corresponding to a marine terrace of semi-consolidated rock (Tn), mainly clayey sandstone, fine-grained sandstone and coarse-grained sandstone. In the Southern limit of the valley, it is possible identify a contact with colluvial deposits (Qc) from the hillsides. Furthermore, Paleozoic intrusive rock (Pzmg) and Jurassic intrusive rock (Js and Jlv) can be found in the southern limit of the valley [5]. The geology units are depicted in Fig. 1.

A comprehensive research of the distribution of damage to buildings during the earthquake of 2010 is available [3]. According to this study, a common plan topology of residential Chilean construction with reinforced concrete consists of walls configurated to resist gravity and lateral loads. The typical damage observed was "unzipping" bending-compression failures in the shear walls, which tended to concentrate in the lower stories, usually in the vicinity of important vertical irregularities. Most damaged buildings presented high average axial stresses in walls due to gravity loads. This study defined three levels of damage based on the operational conditions of the buildings immediately after the earthquake: damage level I is assigned to buildings with restricted use; damage level II to buildings declared non-habitable; and damage level III to collapsed buildings or with risk of collapse. The approximate locations of the damaged buildings in downtown of Viña del Mar are shown in Fig. 1. It can be noted that almost all buildings are located on a straight line in the Qf unit defining a narrow area of approximately 1 km in length. Only building #2 is not located on this straight line. This anomalous distribution of damage motivates this study.

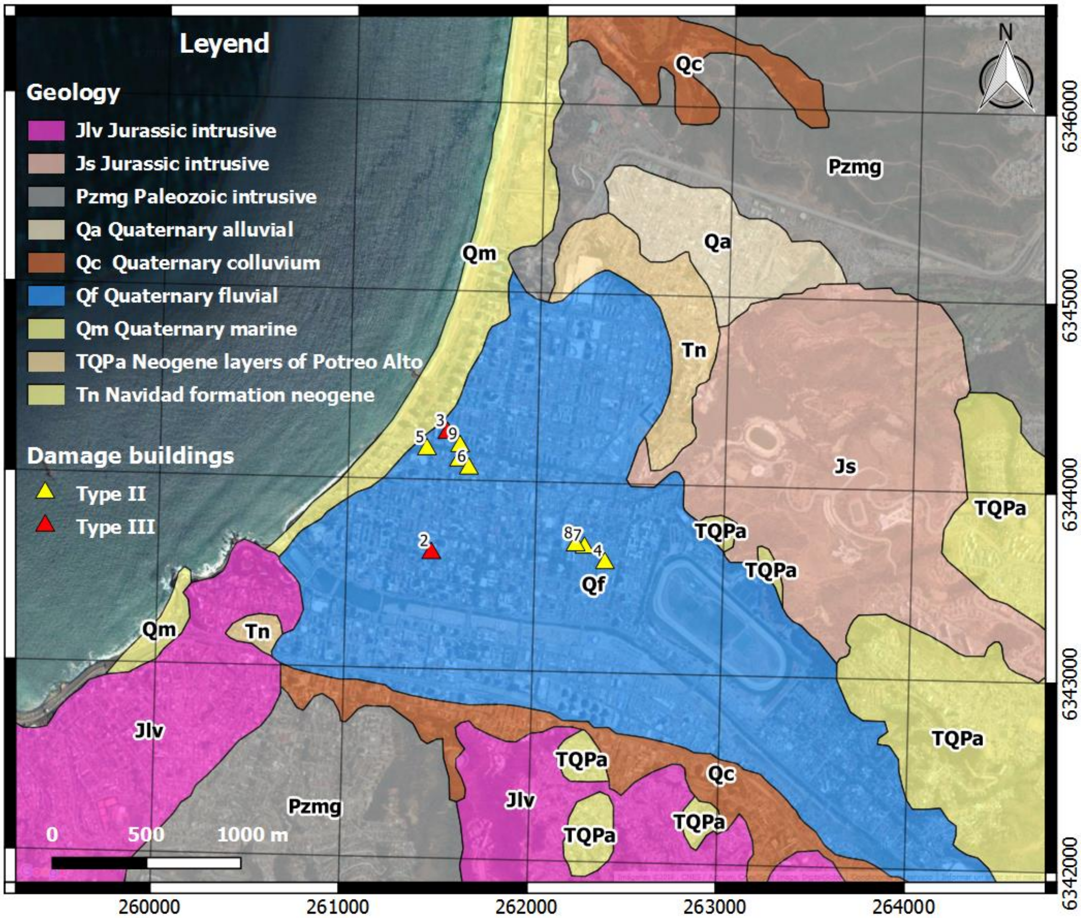

Fig. 1– Geology of the valley and damage buildings. Geology modification of Muñoz (2013).

3. Geophysical Survey description

To characterize the area that concentrates damage to buildings, a detailed geophysical survey was conducted. Details of the techniques used and main hypotheses are presented below.

3.1 Shear wave velocity profiles

We use surface-wave based techniques to obtain Rayleigh wave dispersive properties at several sites in the studied area. By solving an inverse problem, we obtain the shear wave velocity profiles at each location.

In this research, we combine source-controlled (active) with ambient noise (passive) techniques, using sensors arranged in several arrays to capture different wavelengths (Fig. 2). The geometries of the arrays used are:

- Linear array of twenty-four vertical geophones of 4.5 Hz and 1.5 meters interspacing for active measurements.
- Linear array with twelve vertical geophones of 1 Hz and 9 meters of interspacing for passive measurements.
- 2D array with six wireless 3-component geophones using variable spacing oriented with GPS for passive measurements.

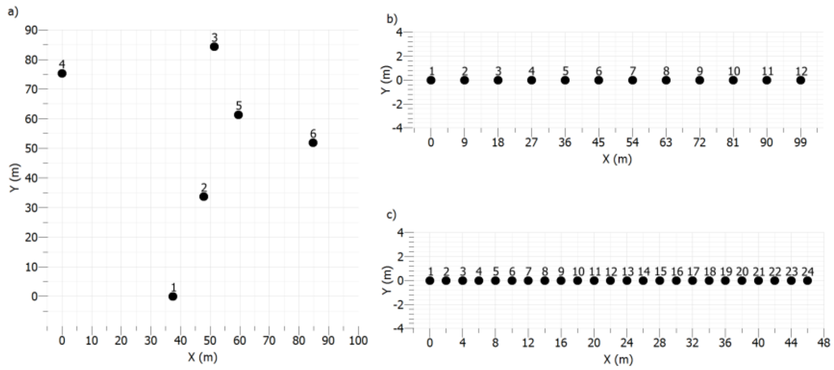

Fig. 2– Types of arrays. a) 2D GPS array. b) Lineal array of 99 m length. c) Lineal array of 46 m length.

We used two type of equipment: a Geometrics® Geode-24 seismograph with twenty-four channels for the linear arrays and six Tromino® 3G for the 2D arrays.

The methodology to combine different analysis techniques to find a reliable shear wave profile was previously proposed in different studies [6]. Frequency-wave number method (FK) [9] has been used for active experiments and 2D arrays. The SPAC method [10] was also used to analyze 2D passive measurements. The Extended Spatial Autocorrelation Method (ESPAC) [12] was selected as the analysis methodology for passive linear measurements.

With the purpose of obtaining the best and deepest shear wave velocity profile; we combined the different dispersion curves to extend the characterization of the site across a wide band of frequencies. An example of the combined dispersion curve is depicted in Fig. 3a.

The inversion process was conducted with the neighborhood algorithm [13]. The inversion process minimizes iteratively the misfit between the empirical dispersion curve and an analytical model. This misfit parameter is defined as:

$$\text{Misfit} = \sqrt{\sum_{i=1}^{n_F} \frac{\left(x_{d,i} - x_{c,i}\right)^2}{\sigma_i n_F}} \tag{1}$$

where, $x_{d,i}$ is the empirical phase velocity, $x_{c,i}$ is the analytical phase velocity, σ_i is the standard deviation of the empirical data and n_F is the total number of i frequency samples. In this study, the minimal misfit obtained was about 0.05. The combined dispersion with the best- adjusted curve is depicted in Fig. 3a, and the corresponding shear-wave velocity profile is depicted in Fig. 3b.

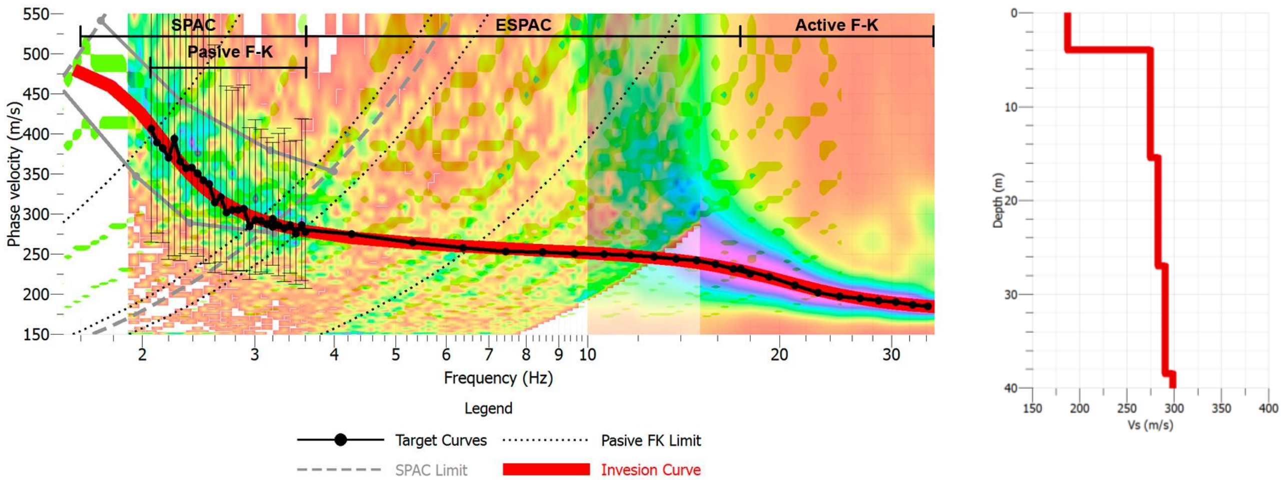

Fig. 3 (a) Combined dispersion curve with the best analytical model for the building N°3 in Fig. 1. (b) Shear wave velocity profile associated with the best inversion.

3.2 Predominant frequencies using horizontal to vertical spectral ratio

Other methodology used in this research was the horizontal to vertical spectral ratio (HVSR) from microtremors (man-made ambient noise) or the Nakamura method [14].

We used a 3-component, 4.5 Hz Tromino® instrument to perform the measurements through the studied area. At each point, we recorded the velocity from ambient noise for a duration of at least 16 min. The analysis procedure was based on [15]; hence, we divided the data in 60 seconds windows to calculate the Stockwell Transform (S-Transform) [16] of each component; both horizontals components were combined to finally compute the horizontal to vertical ratio. A typical result of this methodology is shown in Fig. 4.

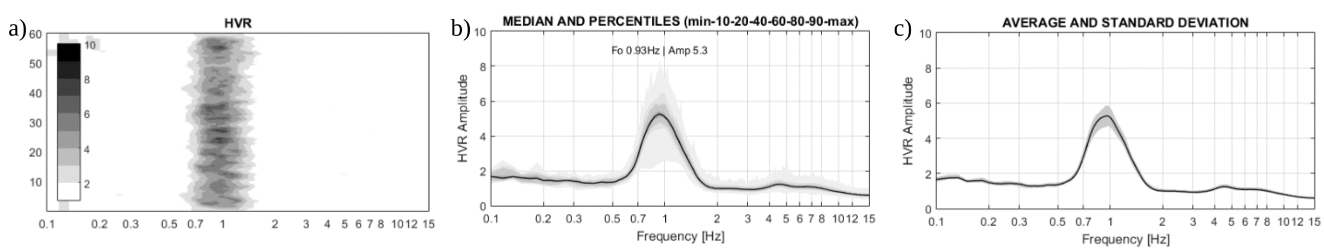

Fig. 4 An example of Nakamura measurement, performed at Viña del Mar, with a large amplitude and 0.93 Hz of frequency. a) HVSR for each 1 min time window, being the grayscale proportional to HVSR amplitude. b) minimum, 10, 20, 40, 60, 50, 80 and 90 percentiles and maximum of HVSR. c) average and standard deviation of HVSR.

3.3 Gravimetry

To obtain information of sediments' thickness variation over the basement, a gravimetric survey was performed across the studied area. Gravity information has been obtained using a Scintrex CG5 instrument and a differential GPS Trimble C5. In terms of accuracy, for gravimetric measurements we obtain errors of about 0.1 mGal and altitude errors below than 50 cm with the GPS base station in Valparaiso have been reached. To estimate the regional field in a continental-scale, we used the density model of South America [17] as the first regional field. Then, we estimated a local regional field with three rock point measurements, where we drew a plane as first approximation to this research. Details of the results obtained are presented below.

4. Geophysical Results and Geotechnical model

The geophysical survey was initially focused on the buildings damaged during the 2010 Chile earthquake. In total, we obtained seven shear wave velocity profiles; 4 were very close to the most damaged buildings and 3 others complete the characterization of the area. Fig. 5a displays the representative location of measurements and the corresponding Vs30 values. It can be noted that Vs30 values are almost uniform through the downtown of Viña del Mar. Nakamura's measurements form a grid in the area with approximately two blocks of interspacing. The results obtained are displayed in Fig. 5b with a double scale; color is proportional to predominant frequency/period (F_0 or T_0), while the size of the symbol is proportional to HVR maximum amplitude. Locations with associated predominant frequencies larger than 2.5 Hz are indicated in white. It should be noted that low frequencies are in the center of the area and the high frequencies are in the edges; in addition amplitudes are fairly homogeneous, suggesting an almost constant impedance contrast between shallow sediments and deep stiffer material.

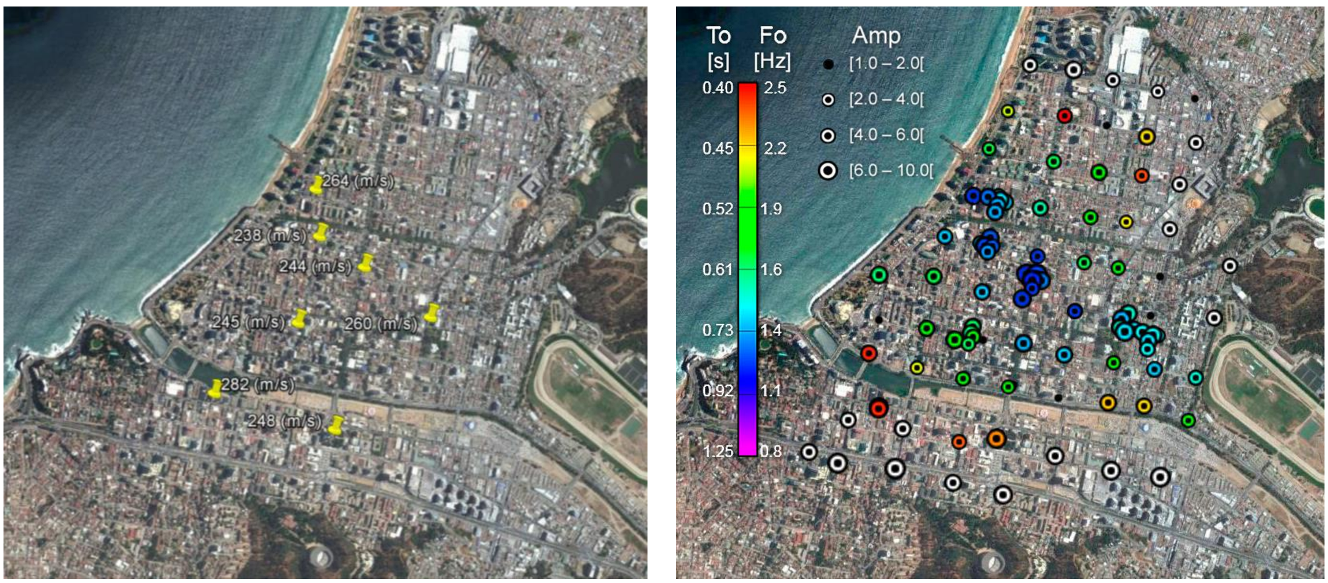

Fig. 5– (a) Approximate location of shear wave velocity profiles and Vs_{30}; (b) Nakamura measurements.

Approximately the same grid of HVSR data is used for gravimetric measurements. The residual of the process described previously is shown in Fig. 6a. Residual gravimetric values against predominant periods T_0 are shown in Fig. 6b. A very good correlation between both quantities can be noted, suggesting that a simple geotechnical model composed by an almost homogenous soil over a stiffer material (apparent bedrock) could explain both sets of data satisfactorily. A similar conclusion has been reported in previous studies [2] based only on Nakamura results, geotechnical boreholes and shear-wave profiles of about 30m depth. Based on this interpretation and the relative uniformity of shear-wave profiles, we fit a curve (Eq. 2) to available shear wave velocity profiles up to one half of the maximum characterized wavelength (Fig. 7a):

$$\mathrm{Vs}(z) = 158.62\, z^{0.2} [\mathrm{m/s}] \tag{2}$$

where z is the depth from surface in meters. The adjusted Pearson correlation coefficient was 0.88.

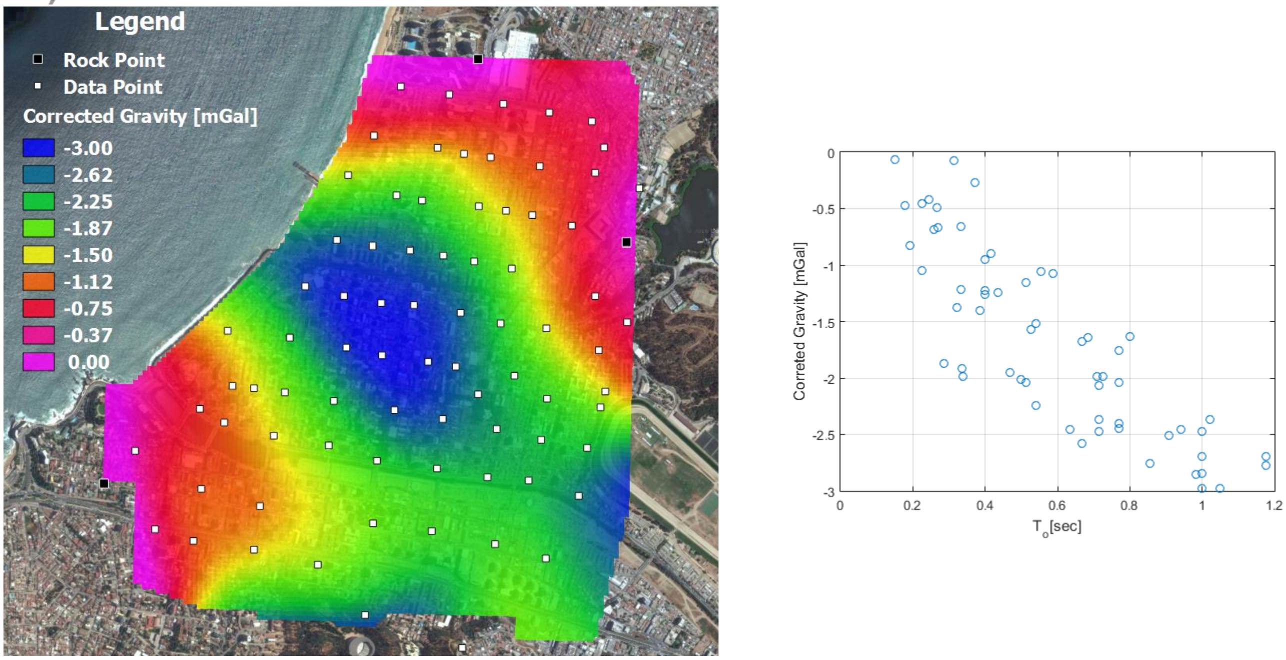

Fig. 6– (a) Approximate location of gravimetric measurement and contours of gravimetric residual values; (b) Correlation between gravimetric residuals and predominant period.

Because it was not possible obtain the exact location of stiffer material (apparent bedrock) with the shear wave profiles, we decided to use the measured predominant frequencies to extend a soil column iteratively down to the longest period of the analytical elastic transfer function that matches the measured value. The shear wave velocity function of Eq. (2) has been used during this process. The soil's density was fixed at 1700 kg/m^3. The apparent bedrock levels obtained are shown in Fig. 7b. We decided to use the gravimetric data only as a qualitative comparison, because direct inversion of residual is highly sensitive to density contrast between soil and apparent bedrock and we do not have reliable information for these values.

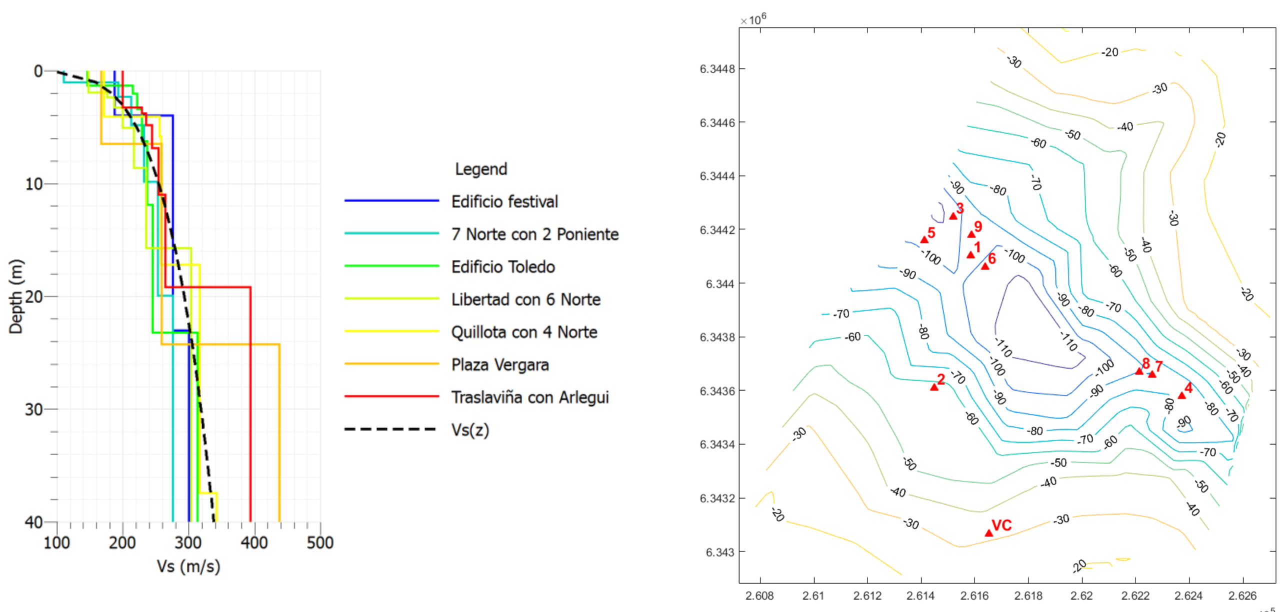

Fig. 7– (a) Shear wave profiles and adjusted curve from Eq. (2); (b) Basement depth from extended profiles based on predominant frequencies.

5. Model settings

The main objective of this research is the numerical evaluation of 3D site effects in the center of Viña del Mar. To model these effects for vertical incident shear waves, we used the spectral element method (SEM), which has shown to be reliable in solving three-dimensional wave propagation problems in heterogeneous media. This method, like the finite element method (FEM), solves the weak formulation of the motion equations, but the main difference is the use of high-order Lagrange interpolants in the functions of the elements and then, use the same quadrature points for integration. This advantage reduces the processing time and the spectral nodes required to characterize the minimum wavelength. For this particular case, the SEM domain ($\Omega \subset \mathbb{R}^3$) considers an elastic medium with a boundary ($\Gamma = \partial\Omega$), which is divided in three for the model:

- Γ_d: Dirichlet conditions are prescribed in the lateral limits.
- Γ_N: External surface load or Neumann conditions in the top (free field).
- Γ_{NR}: Non-reflecting absorbing boundary condition at the bottom.

For purposes of this investigation, we use the implementation described above in SPEED code [20]. This code introduces a forces time history able to generate a displacement in time to include seismic incoming motion.

The model was rotated 18.5º northeast and bounded to include all the relevant available information. The top of the model was the surface topography acquired with the differential GPS. The basement depth obtained above was also included to generate the mesh with the commercial software Trelis®. The grid was spaced in x-y squares of 20x20 m approximately, and across vertical direction, a variable height was used to have six hexahedral elements between the surface and basement. Then, we projected the basement to a flat surface and added another auxiliary layer of hex elements to place the motion input. To cut down the running time at this stage of the investigation, we use a Ricker wavelet with a central period of 0.5 seconds, 1g of maximum amplitude and 5 seconds of duration (Fig. 8). The frequency content of this input signal is compatible with the Chilean earthquake.

To assign the soil materials properties, Eq. (2) has been evaluated at the center of each element to obtain the corresponding value of shear wave velocity. For the basement and the auxiliary layer, a shear wave velocity of 2000 m/s has been assumed. For the elastic properties, we fix the Poisson's modulus at 0.25 and other properties was derived from Vs value. The resulting model with 37800 hex elements, 43350 nodes and 2.506.269 spectral nodes is depicted in Fig. 9.

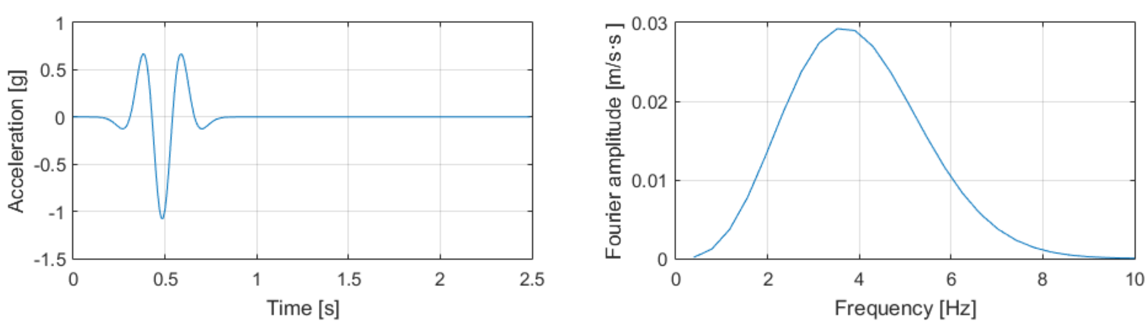

Fig. 8– a) Input Ricker wavelet for the model and b) Fourier amplitude spectrum.

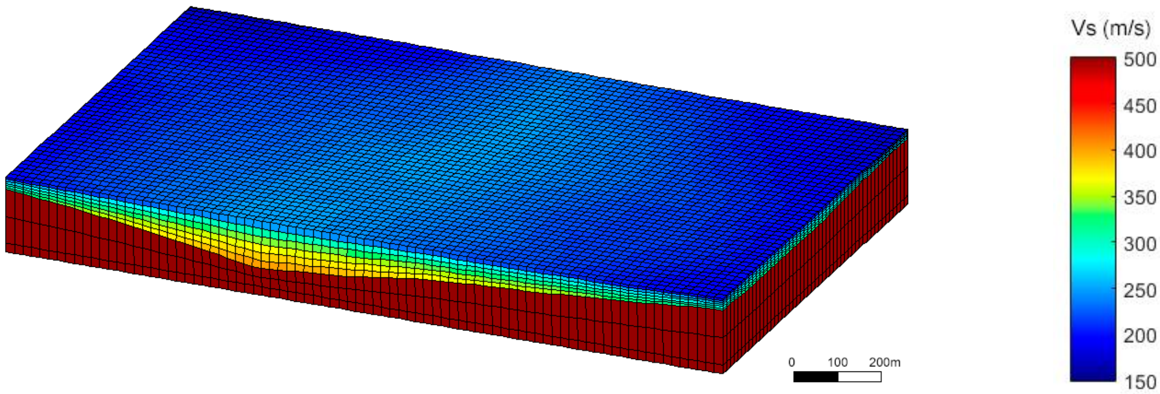

Fig. 9– 3D Model of the studied area of Viña del Mar downtown. The color is proportional to the shear wave velocity in m/s, except the basement Vs, which is 2000 m/s.

6. Model results

At this stage of the research, only the viscoelastic behavior of materials has been considered. The quality factor of the materials has been adjusted to have an approximately constant damping ratio of 1% in the frequency range of interest. The Peak Ground Accelerations (PGA) of the model for a perfectly vertically incident SH wave polarized on the x-axis and y-axis is depicted in Fig. 10. In general, it shows the important influence of the basement shape in the PGA. The deep area of the basin is characterized by a PGA value ranging from 2.8g to 3.2g, i.e. approximately three times the acceleration at basement level. Shallow areas of the basin exhibit PGA values ranging from 2.0g to 2.6g. Some local high values can be noted in the corners of the mesh, but they are probably related to boundary effects. A local increase of accelerations could be noted close to buildings number 7 and 8, where contours of the basement level suggest the location of a narrow canyon. This local increase is more pronounced for the x-axis incoming wave.

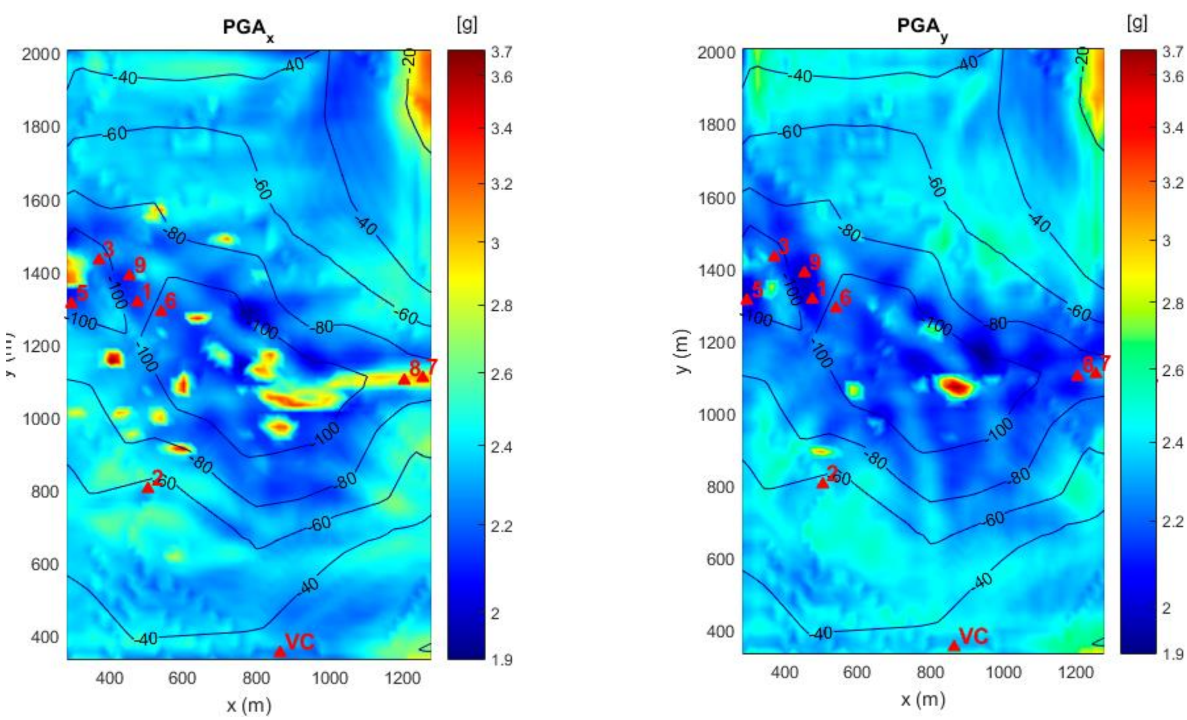

Fig. 10–PGA in x-axis(a) and y-axis(b) for the surface nodes; in red the damaged buildings (for more info. please see Fig. 1) and the basin level contours. The color is proportional to the PGA.

To assess possible three-dimensional site effects, we generated 1D horizontally layered columns (Fig. 11). These columns were chosen according to the buildings observed with the most damage and were analyzed under the same assumptions than the 3D model. The comparison between the 3D model and the associated columns in these three locations (1D standard wave propagation) are depicted in Fig. 12 and Fig. 13. For building 2 and 3, no evidence of important 3D site effects was found and standard 1D wave propagation theory produces similar values as the 3D model. Nevertheless, for building 8, the 3D pseudo-acceleration response spectra considerable differs from 1D propagation. Indeed, in the building 8 for the x-axis input, a significant increase of spectral ordinates can be noted in the range below 0.3s and for the y-axis input, the spectral range periods are slightly expanded compared to the column. Hence, usual 1D vertical wave propagation theory cannot appropriately reproduce seismic amplification in this area. This result might explain the concentration of damage in this area, but realistic soil behavior and input motion must be considered to fully explain this damage distribution.

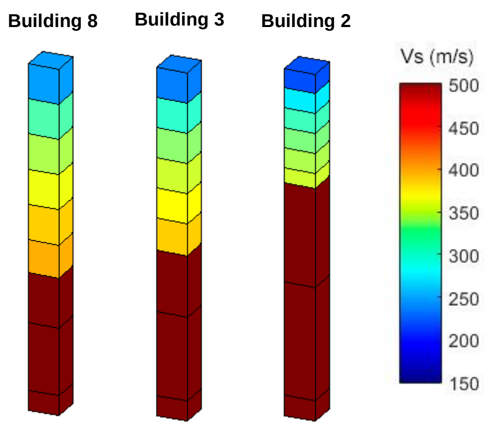

Fig. 11–3D column layered horizontal. The color is proportional to the shear wave in m/s.

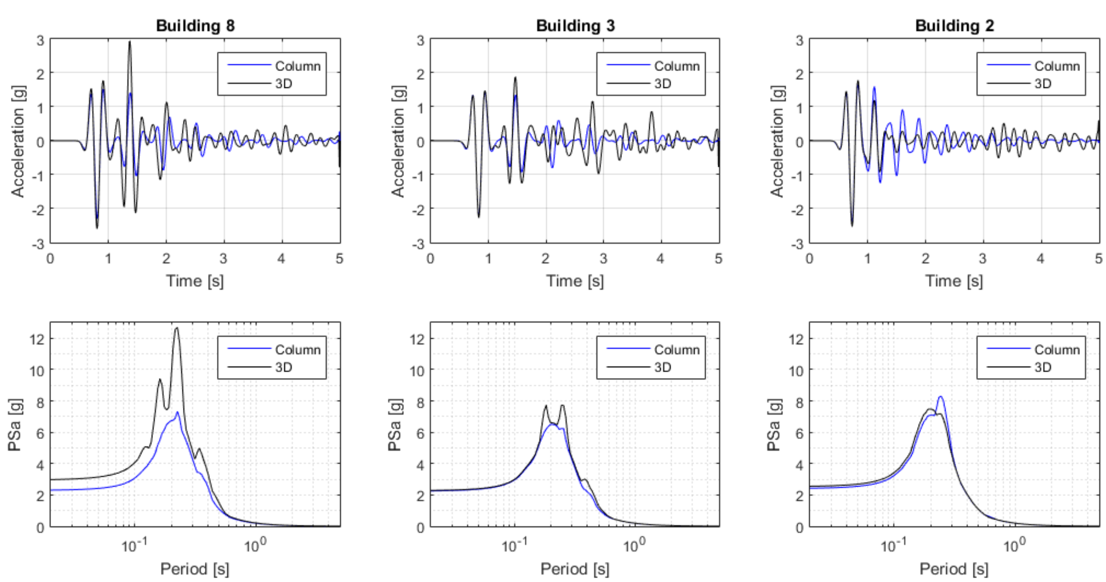

Fig. 12–On top, the acceleration v/s time comparison between the column and the 3D model with input in x-axis; below, the pseudo acceleration response spectra with 5% of damping comparison.

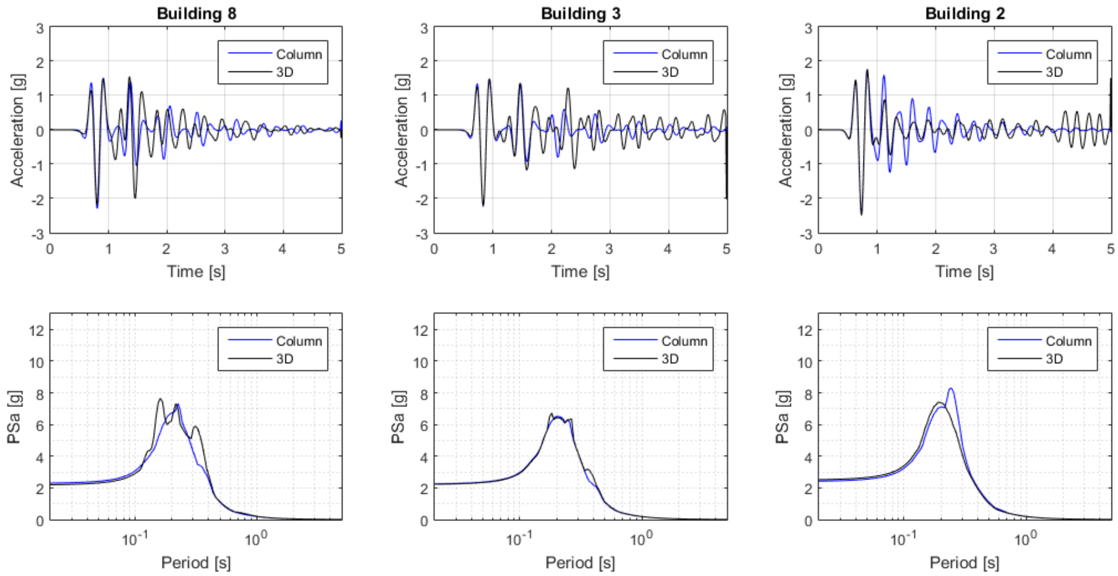

Fig. 13–On top, the acceleration v/s time comparison between the column and the 3D model with input in y-axis; below, the pseudo spectra acceleration with 5% of damping comparison.

7. Conclusions and future work

In this research, based on the 3D modeling of the basin of the downtown area of Viña del Mar city, we found that the shape of the basement could probably induce 3D site effects in an area that concentrates damage for the February 27, 2010 earthquake. The distribution of PGA for this case indicates that standard 30m-depth site classification cannot fully capture local variations of associated surface accelerations. Taking into consideration the geological context and the morphology of the site, the use of 3D numerical simulation provides useful information regarding the possible effects of basin shape in the effective ground motion at the surface.

For future work, we will focus on the non-linearity of the materials and we will consider realistic input motions which need to be included to more accurately evaluate the probable ground motion amplification and 3D site effects. Indeed, available records at Viña Centro (VCN station) suggest that inelastic behavior of soils could play a significant role in the observed surface motion in the city. Both issues, inelastic soil behavior and realistic motions, are part of the ongoing work of this research.

8. References

[1] Madariaga, R., 1998. Sismicidad de Chile. Física de la Tierra, Issue 10, pp. 221-258.

[2] Thorson, R., 1999. La falla Marga Marga. Viña del Mar. Departamento de Obras Civiles. Universidad Técnica Federico Santa María.

[3] Jünemann, R., De La Llera, J., Hube, M. and Kausel, E. (2015). A statistical analysis of reinforced concrete wall buildings damaged during the 2010, Chile earthquake. Engineering Structures, 82, pp168-185.

[4] Chavez-Garcia FJ, Cuenca J (1998) Site effects and microzonation in Acapulco. Earthq Spectra 14(1), pp. 75–93.

[5] Muñoz, E., (2013). Susceptibilidad de remociones en masa y de respuesta sísmica asociada a fallas mayores en zonas urbanas. estudio de caso en viña del mar, V región. Tesis para optar al grado de magister en ciencias mención geología. Universidad de Chile.

[6] Tokimatsu, K., (1997). Geotechnical site characterization using surface waves. In: Proceedings of 1st international conference on earthquake geotechnical engineering, vol 3, pp 1333–1368

[7] Humire, F., Saéz, E., Leyton, F. and Yañez, G., (2015). Combining active and passive multi-channel analysis of surface waves to improve reliability of vs30 estimation using standard equipment. Bull Earthq Eng 13(5):1303–1321.

[8] Becerra, A., (2015). Seismic microzoning of Arica and Iquique, Chile. Thesis to obtain the degree of Master of Science in Engineering. Pontificia Universidad Católica de Chile.

[9] Kvaerna, T., Ringdahl, F., (1986). Stability of various fk estimation techniques. Norsar Semiannu Tech Summ 1:1–86.

[10] Aki, K. (1957), Space and time spectra of stationary stochastic waves, with special reference to microtremors. Bull. Earthq. Res. Inst., Tokyo Univ., 35:415-456.

[11] Bettig B., Bard, P., Scherbaum, F., Riepl, J., Cotton, F., Cornou, C., Hatzfeld, D., (2001). Analysis of dense array noise measurements using the modified spatial auto-correlation method (SPAC): application to the grenoble area. Boll Geofis Teor Appl 42(3–4):281–304.

[12] Hayashi K. (2008). Development of the Surface-wave Methods and Its Application to Site Investigations. Ph.D Dissertation, Kyoto University, 2008.

[13] Wathelet, M., (2008). An improved neighborhood algorithm: parameter conditions and dynamic scaling. Geophys Res Lett 35(9): L09301.

[14] Nakamura, Y. (1989). A method for dynamic characteristics estimations of subsurface using microtremors on the ground surface. Q. Rep. Railway Tech. Res. Inst. Japan 30, 25-33.

[15] Leyton, F., Ramírez, S. & Vásquez, A., 2012. Uso y limitaciones de la Técnica de Nakamura en la clasificación sísmica de suelos. Congreso Chileno de Geotecnia, Volume VII.

[16] Stockwell, R., A basis for efficient representation of the S-transform, Digital Signal Processing, vol. 17, no. 1, (2007), pp. 371-393.

[17] Tassara, A.; Götze, H.; Schmidt, S.; Hackney, R. 2006. Three dimensional density model of the Nazca plate and the Andean continental margin. Journal of Geophysical Research: Solid Earth 111 (B09404). doi:10.1029/2005JB003976.

[18] Verdugo, A., 1995. Estudio geofísico de los suelos de fundación para una zonificación sísmica de Valparaíso y Viña del Mar. Memoria para optar al título de Ingeniero Civil. Universidad de Chile.

[19] Carrasco, O. & Núñez, C., 2013.Microzonificación sísmica de la ciudad de Viña del Mar. Memoria para optar al título de ingeniero Civil, Universidad Técnica Federico Santa María.

[20] Antonietti, P. F., Mazzieri, I., Quarteroni, A., & Rapetti, F. (2012). Non-conforming high order approximations of the elastodynamics equation. Computer Methods in Applied Mechanics and Engineering, 209-212, 212–238.